INFLUENCE OF SiO_2-BASED ELECTROLYTE ON THE CORROSION RESISTANCE OF PEO COATINGS ON TITANIUM

VLĂDUȚ ION, OANA ALICE RUSU

Institute for Nuclear Research (RATEN ICN) Piteşti, Romania
e-mail: oana.rusu@nuclear.ro

Abstract

This paper presents the results obtained from treating grade 2 titanium samples in electrolytic plasma in an aqueous electrolyte containing various types of SiO_2, under pulsed galvanostatic conditions. The objectives included obtaining coating thickness, examining their morphology and acquiring corrosion curves. The aim of these investigations was to identify the influence of the type of SiO_2 used in plasma electrolytic oxidation (PEO) on the corrosion resistance of the resulting coatings.

Keywords: *PEO, SEM, Coating thickness, Corrosion, SiO_2*

Introduction

The development of small modular reactors as well as prolonged lifetime of existing nuclear power plants call for new materials utilizable in the extreme conditions of nuclear reactors.

Titanium and its alloys are of great interest in advanced engineering applications due to their superior characteristics such as high strength-to-weight ratio, good corrosion resistance, high temperature resistance etc. [1]. Titanium's strength to handle high-stress and hostile environments make it an ideal metal for the rigors of power generation and is seeing a greater demand in this industry.

The strength of titanium is similar to steel, but its density is about half that of steel, and compared with aluminium, titanium is five times stronger [2]. It was shown [3] that Ti alloys are highly radiation resistant. At temperatures below 500 °C, void swelling, which is the dominant mechanism of radiation damage in 316SS and other candidate materials, is either non-existent or negligible in titanium alloys. Moreover, Ti-70Al and Ti-6Al-4V were more resistant to helium embrittlement than 316SS. A Ti component will cause only minor radiological hazard 8 years after reactor shutdown and will, therefore, reduce the waste disposal costs/concerns from reactor systems. In comparison, a 316SS component will be 23,000 times more radioactive after 8 years. A recent work investigated the influence of neutron irradiation on the microstructure and related mechanical properties of Ti Grade 2 [4]. Condenser piping made from Ti is becoming highly sought after in the construction of power plants for its much greater lifespan versus more traditional metals in harsh environments [5]. Titanium is also an ideal metal for the nuclear waste storage containers due to its low reactivity to other elements and resistance to corrosion. This gives such Ti made containers a greatly increased lifespan, compared to other materials. A recent work has reviewed the corrosion performance of Ti alloys for the current WP design at Yucca Mountain under repository environmental conditions [6]. The review concentrates on potential corrosion processes possible in aqueous environments. With respect to the Ti Grade 7 drip shields used in the Yucca Mountain repository, general corrosion, hydrogen induced cracking, and radiation-assisted corrosion will not lead to failure within the 10,000 year regulatory period.

Research works [7-9] have proved that titanium alloys could be good candidates for nuclear Pressurised Water Reactor (PWR) primary circuit structure components. They could indeed replace some stainless steel parts because of their lower neutron activation and their good mechanical properties.

Thus, with gradual increasing applications, the corrosion of Ti alloys has attracted great attention. The dense passive oxide, formed on the surface of titanium alloys in an oxygen-containing environment due to the high affinity of Ti and oxygen, has the property of self-healing. But, when the passive film is destroyed and the base metal is exposed in the oxygen-containing corrosive solutions, the dissolved Ti ions will quickly react with oxygen to from a new oxide film, again separating the base metal from the corrosive media. However, when titanium alloys are used in strong reducing acids or oxygen-deficient anhydrous environments, especially under high temperature conditions, once the passive film is damaged, the self-healing will be difficult and corrosion will occur. Thus, a possible way to increase the natural thickness of TiO_2 is by surface treatments. Oxidation treatments, specifically anodization, have been considered to tune the TiO_2 layer in order to increase its thickness and the pure Ti corrosion resistance up to the level of more expensive alloys [10]. Nowadays, plasma electrolytic technologies, as a progression of traditional anodizing into the higher voltages, enable production of oxide ceramic coatings on Ti surfaces to address the growing demand in corrosion and erosion resistance and other desired surface properties [11].

Plasma Electrolytic Oxidation (PEO) is an environmentally friendly and economically viable, widely used in obtaining oxide coatings, cleaning metal surfaces, carburizing, nitriding and oxidation. Layers produced by electrolytic plasma oxidation exhibit excellent adhesion to the substrate, high hardness, wear resistance and corrosion resistance, and they are good conductors of electricity. Moreover, this process which produces layers with a wide range of functional properties, has a minimal effect on the mechanical properties of the substrate material (affecting it insignificantly due to slight heating) [12, 13].

By selecting and properly controlling the parameters of the PEO process (current density, electrolyte temperature, electrolyte concentration etc.), it is possible to exert some control over the thickness, composition, morphology and hardness of the oxide layer [14, 15].

Experimental

Cylindrical Ti Grade 2 coupons cut from a Ti Grade 2 Bar (Grade R50400, C-0.08, O-0.25, N-0.03, H-0.015, Fe-0.3), ASTM B348 Ø 25 x 150 mm, were degreased with acetone, rinsed with distilled water, and air-dried. The coupons were connected to the positive pole (anode) of the power source via Ti Grade 2 rods. The rods were insulated using Teflon and insulating varnish so that only the coupons surface came into contact with the electrolyte. The coupon was fully immersed in the electrolyte and after each experiment, it was rinsed with distilled water and air-dried. A programmable DC power source of type EA-PS 8400-70 was used. As the cathode, a stainless steel cubic electrolysis vessel, connected to the negative pole, was used. The tests were conducted under pulsed galvanostatic conditions, maintaining the same current density and duty cycle. Magnetic stirring at approximately 200 rpm was employed. For the experiments electrolytes containing Na_2SiO_3 : KOH (1:4) were prepared, using different types of SiO_2 sources:

1. Sodium silicate solution extra pure (Merck) - used for *Exp1 coupon*;
2. Sodium silicate powder (Fisher Scientific) - used for *Exp2 coupon*;
3. LUDOX HS-40 colloidal silica (Sigma Aldrich) - used for *Exp3 coupon*.

The characterization techniques used included metallographic microscopy and Scanning Electron Microscopy (SEM). Metallographic examination of the coupons was performed using an OLYMPUS GX 71 optical microscope. To determine the coating's thickness, the samples were cross cut and embedded in thermoplastic copper resin using an automatic press, before being polished to 1200 grit. SEM observations were conducted using the TESCAN VEGA II LMU microscope operating at 30 kV. Corrosion resistance was determined using potentiodynamic polarization. Potentiodynamic polarization measurements were carried out in a 3.5% NaCl aqueous solution. The equipment used consisted of a conventional electrochemical cell connected to a Parstat 2273 potentiostat. The Tafel slopes method was employed.

All polarization measurements were conducted using the Power Suite software package. After stabilizing the electrochemical system, the potentiodynamic polarization curve was recorded for each coupon starting from -0.5 V vs. open circuit potential and going up to +2 V vs. open circuit potential, with a scan rate of 1 mV/s.

Results and discussions

The thickness of the layers developed on the coupons *Exp1, Exp2, Exp3* was measured using an optical microscope and the values are presented in Table 1.

Table 1. Thicknesses of the layers recorded for Ti Grade 2 coupons treated with PEO in the aqueous electrolyte Na_2SiO_3 : KOH (1:4) obtained with different types of silicate (*Solution, Powder and Colloidal*)

No.	Experiment	Layer Thickness [µm]
1	*Exp1*	3.07 – 5.87
2	*Exp2*	2 – 4.40
3	*Exp3*	3.33 – 5.87

Figs 1 to 3 present the coating layers developed on different zones of *Exp1 coupon*. It can be observed that the coating is uniformly distributed over the entire surface of the coupon, with a layer thickness ranging from 2.67 µm to 5.87 µm.

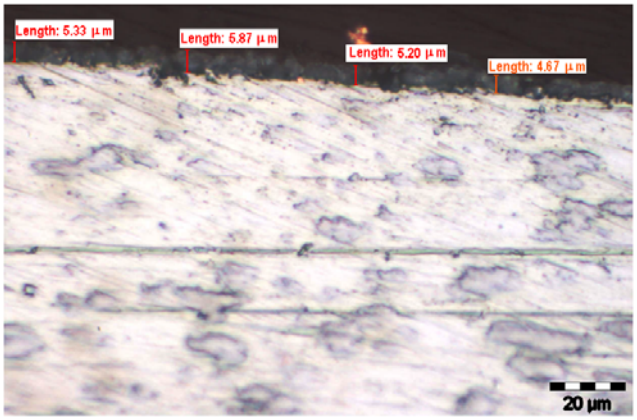


Fig. 1. Optical micrograph of the coating layer obtained on *Exp1* Zone 1 (magnification x 500)

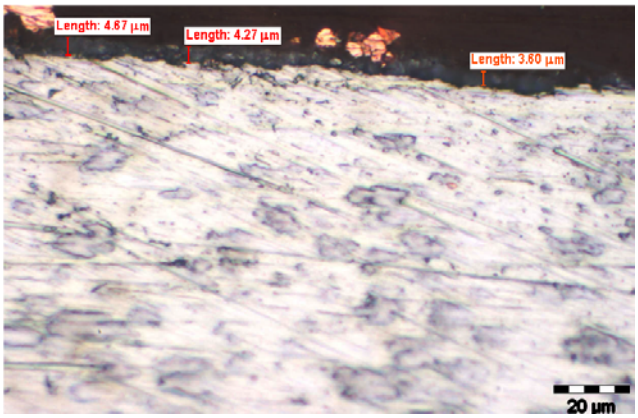


Fig. 2. Optical micrograph of the coating layer obtained on *Exp1* Zone 2 (magnification x 500)

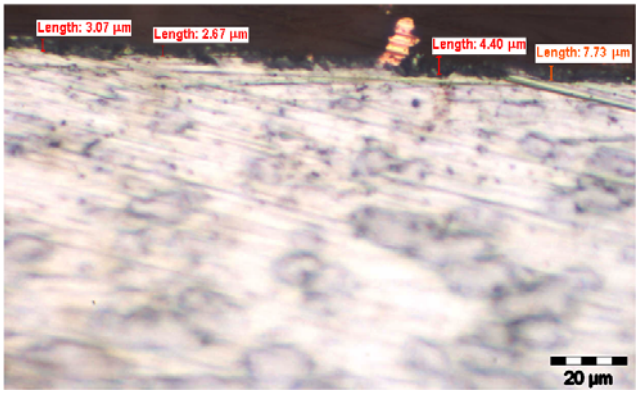


Fig.3. Optical micrograph of the coating layer obtained on *Exp1* Zone 3 (magnification x 500)

Figs. 4 and 5 depict the optical micrographs of the coating layer obtained on the *Exp2 coupon*. It can be noticed that the coating is uniformly distributed over entire surface of the sample. Although both *Exp1* and *Exp2* showed a similar trend, it can be noted that the layer thickness measured for *Exp2* (using powdered silicate) is smaller compared to that measured for the *Exp1 coupon* (using silicate solution).

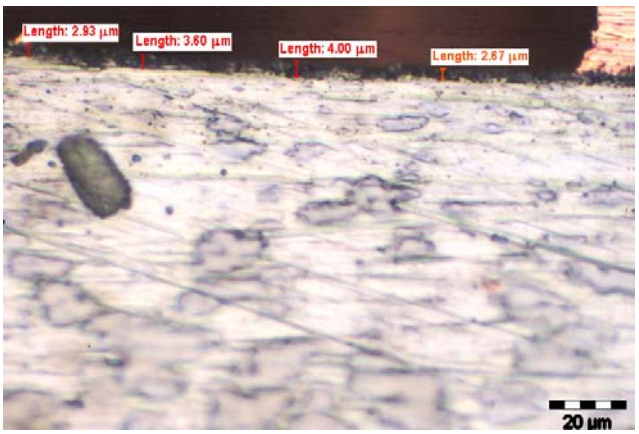


Fig. 4. Optical micrograph of the coating layer obtained on *Exp2* Zone 1 (magnification x 500).

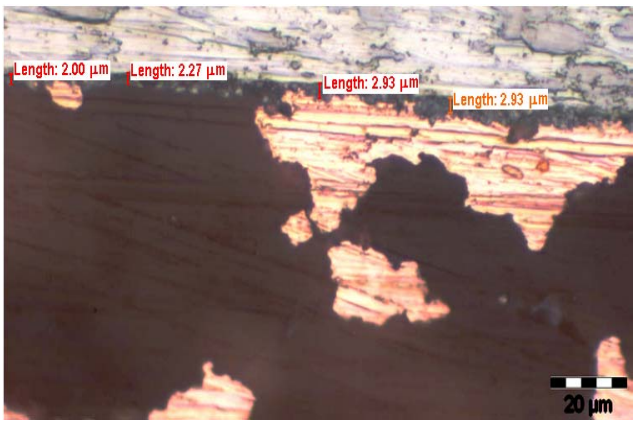


Fig. 5. Optical micrograph of the coating layer obtained on *Exp2* Zone 2 (magnification x 500).

The optical micrographs of the coating layers developed on *Exp3 coupon* are presented in Figs 6 and 7. It can be observed that the coating is uniformly distributed over the entire surface of the coupon.

Although *Exp3* showed a different evolution compared to the other two experiments, it can be noted that the coating layer obtained in the colloidal silicate is much more compact, with minimal variations in thickness, ranging from 3.33 µm to 6 µm.

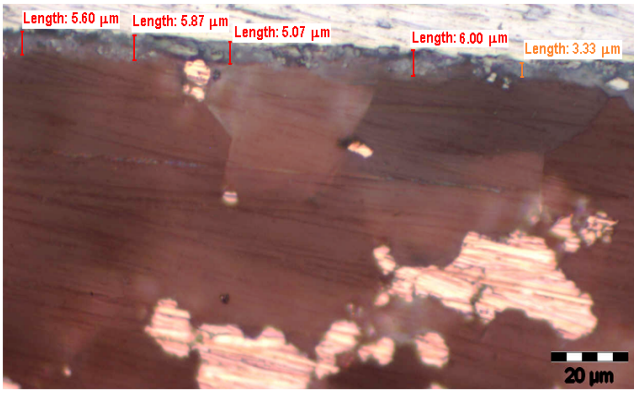


Fig. 6 Optical micrograph of the coating layer obtained on *Exp3* Zone 1 (magnification x 500).

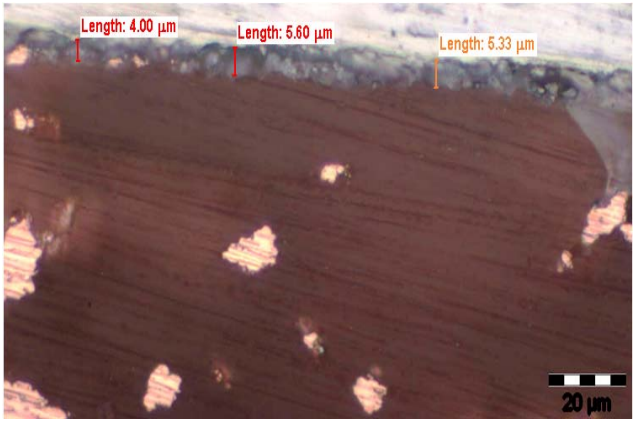


Fig. 7. Optical micrograph of the coating layer obtained on *Exp3* Zone 2 (magnification x 500).

Thus, it is observed that under the studied conditions, the most compact layer thicknesses are obtained in the case of experiments conducted in the silicate solution (*Exp1*) and in the colloidal silicate (*Exp3*), where relatively similar thicknesses were obtained, with small fluctuations in height.

The layer thicknesses obtained are comparable to those reported in the literature under similar conditions. In [16] there were reported thicknesses in the range of 5 – 15 µm on the Ti-6Al-4V alloy using the same electrolytes, but using longer treatment time. It can be assumed that under the considered experimental conditions, increasing the PEO treatment duration led to increased coating's thickness.

In Figs 8 and 9, SEM micrographs obtained on *Exp1 coupon* are highlighted. Two distinct areas were studied: the actual area of the sample (Fig. 9a*)* and the "stained" area of the sample *(*Fig. 9b*)*. The stain's surface exhibits a different microstructure compared to the rest of the sample. It can be observed that the coating on the stain is more porous (crater-like) compared to the rest of the sample and, furthermore, it presents small cracks, suggesting that in this area, the obtained coating is fragile.



Fig. 8. SEM micrograph of the PEO coating on *Exp1 coupon*, normal size

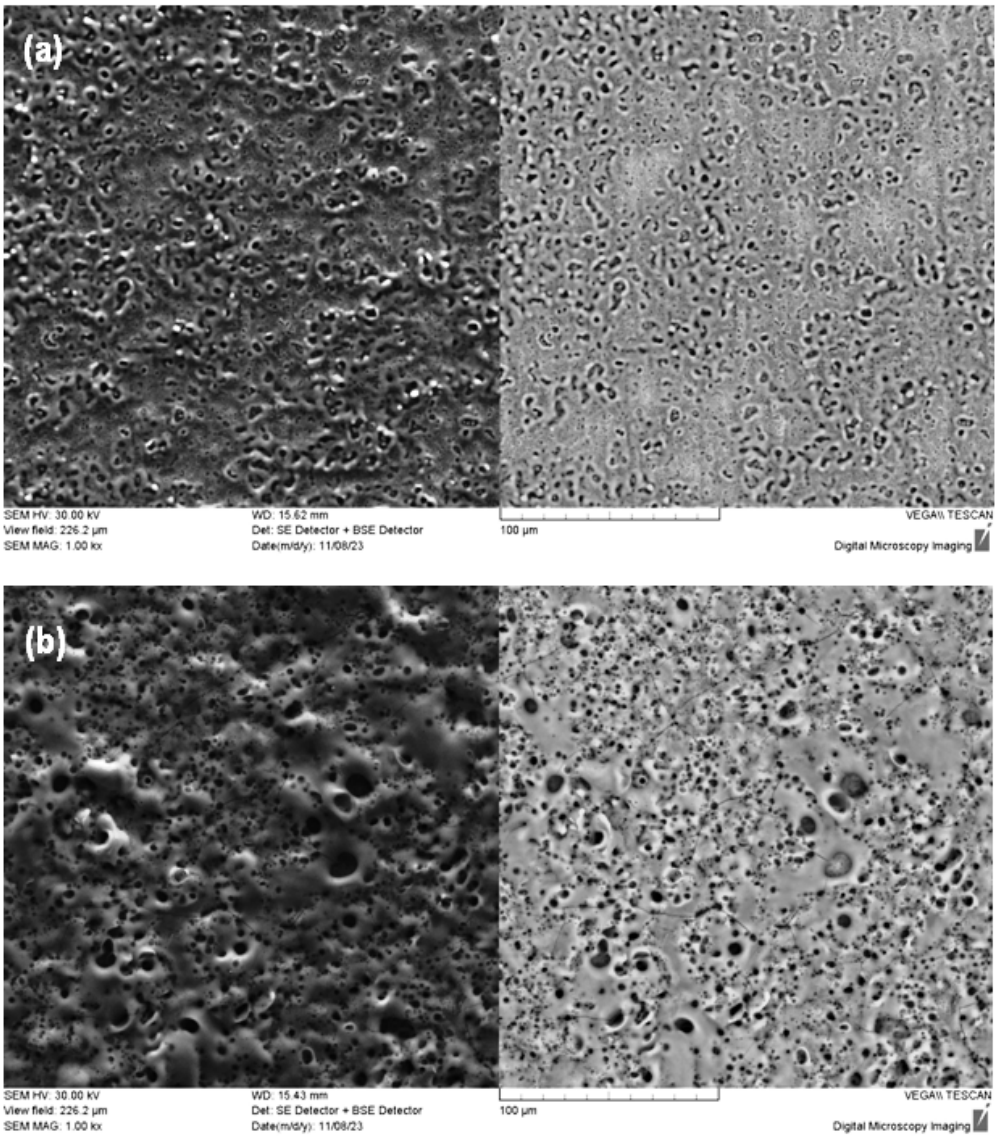


Fig. 9. SEM micrographs of the PEO coating on *Exp1 coupon*, small size ×1 k:
(a) on the main surface and (b) on the stained area of the sample

In Figs 10 and 11, SEM micrographs obtained on *Exp2 sample* are highlighted. Two distinct areas were studied: the actual area of the sample (Fig. 11a) and the "stained" area of the sample (Fig. 11b). It was observed that the surface of the sample is similar to that in the *Exp1 coupon* case (possibly minor differences in crater size), suggesting that although the type of silicate differs (solution vs. powder), the microstructure is similar.

Regarding the stained area of *Exp2 coupon*, it exhibits a different microstructure compared to the rest of the sample and to the stain on *Exp1 coupon*. It can be observed that the coating on the stained area is uneven, showing areas with a different and much more porous structure compared to the rest of the sample.

Additionally, the entire surface of the *Exp2 coupon* exhibits more cracks compared to the *Exp1 coupon*, suggesting a more fragile coating comparatively with the one of *Exp1 coupon*.

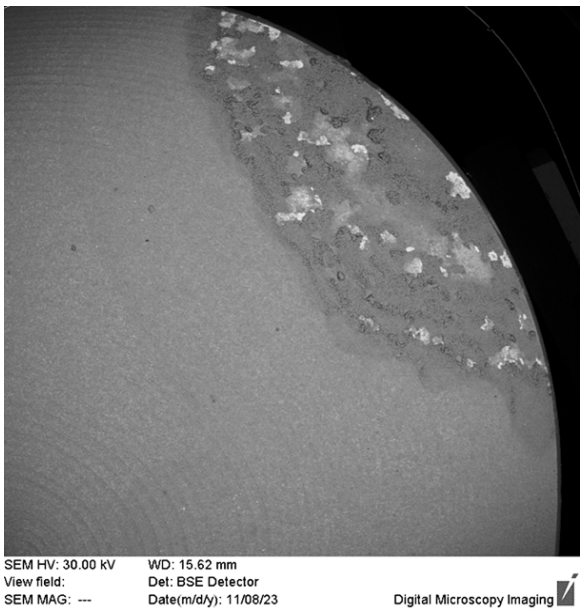


Fig. 10. SEM micrograph of the PEO coating on *Exp2 coupon*, normal size

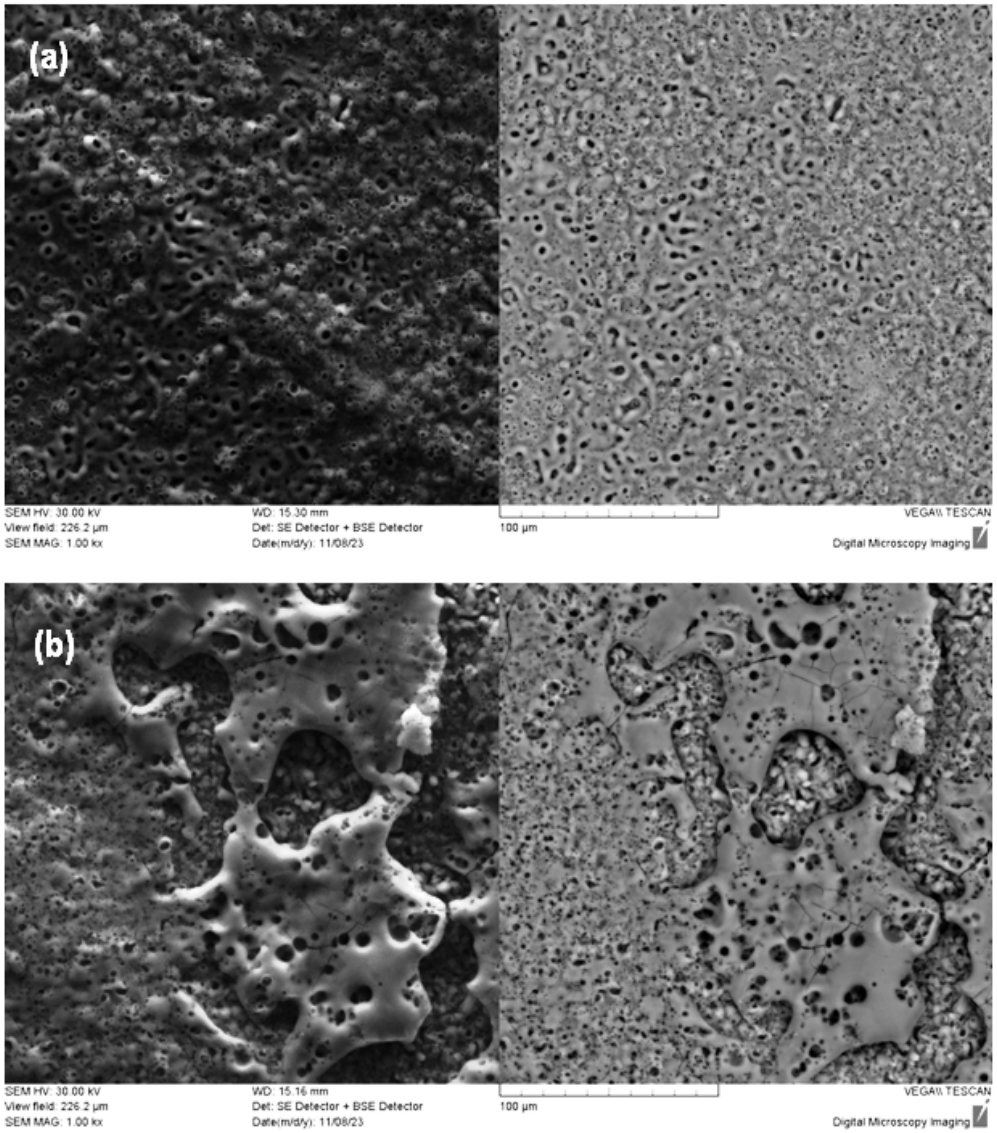


Fig. 11. SEM micrographs of the PEO coating on *Exp2 coupon*, small size ×1 k: (a) on the main surface and (b) on the stained area of the sample

In Fig 12 and 13, SEM micrographs obtained on the surface of *Exp3 coupon* are highlighted. Two distinct areas were analysed: the actual area of the coupon (Fig. 13a) and a "stained" area (Fig. 13b). Unlike coupons *Exp1* and *Exp2*, the surface of *Exp3 coupon* does not differ significantly from the stained area, with both zones exhibiting very similar structures. The coating of *Exp3 coupon* is very uniform (without areas with different structures), the pores are much smaller, and there are no cracks.

To evaluate the corrosion susceptibility of the coated coupons, they were subjected to electrochemical tests. Thus, potentiodynamic polarization tests were performed on coated samples, compared to an uncoated sample. Table 2 presents the electrochemical parameters obtained.

Fig. 14 depicts the potentiodynamic polarization curves plotted for the uncoated coupon and *Exp1*, *Exp2* and *Exp3* coated coupons. The electrochemical parameters (corrosion potential, current density and corrosion rates) were determined using the Tafel slopes intersection method.



Fig. 12. SEM micrograph of the PEO coating on *Exp3 coupon*, normal size

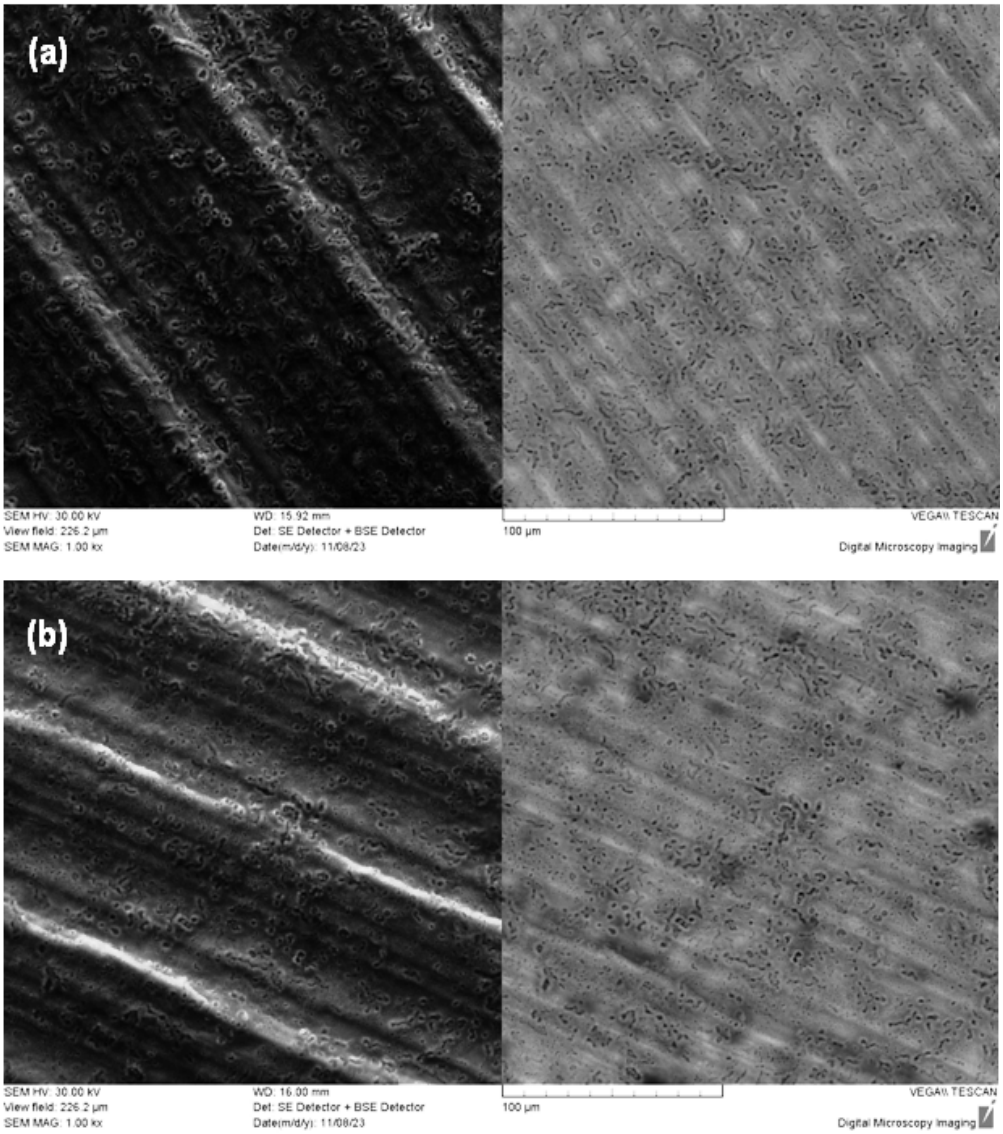


Fig. 13. SEM micrographs of the PEO coating on the *Exp3 coupon*, small size ×1 k:
(a) on the main surface and (b) on the stained area of the sample

Table 2. Electrochemical parameters recorded for coated and uncoated coupons, tested in the aqueous electrolyte Na_2SiO_3 : KOH (1:4) with different types of silicate (Solution, Powder, and Colloidal)

Sample Code	E_{cor} (mV vs. SCE)	I_{cor} [µA]	i [µA/cm^2]	V_{cor} [mmpy]
Ti Substrate	-719	9.980e+000	1.4	1.740e-001
Exp1	-238	2.260e-001	0.4	9.62e-003
Exp2	-310	8.231e-001	0.5	8.102e-002
Exp3	-134	2.700e-002	0.3	2.130e-003

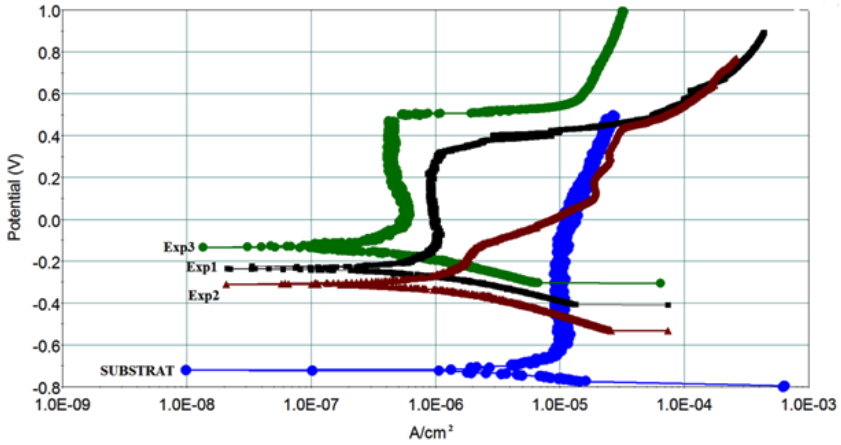


Fig. 14. The potentiodynamic polarization curves, obtained in a 3.5% NaCl aqueous solution for uncoated Ti coupon and the PEO treated samples: *Exp1*, *Exp2* and *Exp3*

The corrosion potential obtained in the case of the untreated Ti substrate is -719V, with a corrosion current density of about 1.4 µA/cm². After PEO treatment, the corrosion potential of all coated coupons shifts to more anodic values, accompanied by a decrease in the corrosion current density (see Fig. 14), indicating an enhancement in corrosion protection.

Therefore, from Table 2 it can be observed that all PEO-coated coupons exhibited significantly lower corrosion current density (I_{cor}) compared to the untreated Ti substrate. Moreover, the protective layers formed by PEO treatment on *Exp3 coupon* demonstrate the best corrosion resistance among all samples, confirmed by the lowest values of I_{cor} and V_{cor}.

Thus, the comparison of PEO-treated Ti with untreated Ti suggests passivation, indicated by a more anodic values of corrosion potential and a significant decrease in the corrosion rate.

This favourable corrosion protection behaviour can be explained by the use of colloidal silicate, which aids in achieving an adherent and less porous coating. In [17], the authors concluded that the use of SiO_2 in coatings on alloys leads to higher stability in corrosive environments, smaller pores, and higher coating density. In [18], the authors suggested that the main reason for the improved corrosion resistance were the highly chemically stable SiO_2 nanoparticles incorporated into the coating during the PEO process.

Conclusions

Based on the results obtained in this study, which are also supported by the specialized literature, it can be stated that the PEO coatings obtained on Titanium Grade 2 samples confer protection against corrosion.

The surface analyses carried out through SEM and optical microscopy confirmed that the coating obtained using silicate in colloidal form, compared to the other types of silicates studied, has a uniform morphology, low porosity, compact microstructure and lack of microcracks.

In conclusion, we can state that in order to obtain uniform, compact, less porous and microcrack-free coatings under the experimental conditions presented in this work, it is recommended to use SiO_2 in colloidal form.

References

[1] Geetha, M., Singh, A.K., Asokamani, R., Gogia, A.K. (2009) ″Ti based biomaterials, the ultimate choice for orthopaedic implants - A review″, *Prog. Mater Sci.*, Vol. 54, pp. 397–425.

[2] Qiu, G., Guo, Y. (2022) ″Current situation and development trend of titanium metal industry in China″, *Intern. Journal of Minerals, Metallurgy and Materials*, Vol. 4, pp. 599-610.

[3] Jones, R.H., Leonard, J., Johnson, J. (1980) ″Assessment of Titanium Alloys for Fusion Reactor First-Wall and Blanket Applications″, Final Report, Battelle Pacific Northwest Labs., USA.

[4] Zhánal, P., Krajnák, T., Zimina, M., Fedoriková, A., Srba, O., Harcuba, P., Stráský, J., Janecek, M. (2022) ″Influence of Neutron Irradiation on Microstructure and Mechanical Properties of Coarse- and Ultrafine-Grained Titanium Grade 2″, *Metals*, Vol. 12(12), paper 2180, https://doi.org/10.3390/met121221802180

[5] Addere Additive Manufacturing ″Titanium in Power Generation & Storage″ https://www.addere.com/materials/titanium/titanium-in-power-generation-storage/

[6] Hua, F., Mon, K., Pasupathi, P., Gordon, G. (2004) ″Corrosion of Ti grade 7 and other Ti alloys in nuclear waste repository environments - A Review″, *NACE Intern. CORROSION*, Paper No. 04689, New Orleans, USA.

[7] Zhang, L., Sun, D., Xiong, R. (2020) ″Study of corrosion kinetics and microstructure of α-phase pure titanium tube in environment 300 °C and 8.6MPa water″, *Corrosion Science*, Vol. 162, p. 108217, https://doi.org/10.1016/j.corsci.2019.108217 .

[8] Bignon, Q., Martin, F., Auzoux, Q., Miserque, F., Tabarant, M., Latu-Romain, L., Wouters, Y. (2019) ″Oxide formation on titanium alloys in primary water of nuclear pressurised water reactor″, *Corrosion Science*, Vol. 150, p. 32-41, http://dx.doi.org/10.1016/j.corsci.2019.01.020

[9] Bignon, Q., Martin, F., Auzoux, Q., Miserque, F., Tabarant, M., Latu-Romain, L., Wouters, Y. (2018) ″Corrosion of titanium alloys in primary water of nuclear pressurised water reactor″, *Corrosion Science,* Vol. 150, pp.32-41, http://dx.doi.org/10.1016/j.corsci.2019.01.020

[10] Prando, D., Brenna, A., Diamanti, M.V., Beretta, S., Bolzoni, F., Ormellese, M., Pedeferri, M.P. (2018) ″Corrosion of titanium: Part 2: Effects of surface treatments″, *Journal of Appl. Biomat. & Functional Materials*, Vol.16(1), pp.3-13.

[11] Aliofkhazraei, M., Macdonald, D.D., Matykina, E., Parfenov, E.V., Egorkin, V.S., Curran, J.A., Troughton, S.C., Sinebryukhov, S.L., Gnedenkov, S.V., Lampke, T., Simchen, S., Nabavi, H.F. (2021) ″Review of plasma electrolytic oxidation of titanium substrates: Mechanism, properties, applications and limitations″, *Applied Surface Science Advances*, Vol. 5, paper 100121.

[12] Hussein, R.O., Northwood, D.O., Nie, X. (2010) ″Coating growth behaviour during the plasma electrolytic oxidation process″, *Journal of Vacuum Science & Techn. A, Vacuum Surfaces and Films*, Vol. 28(4), pp. 766-773.

[13] Wernick, S., Pinner, R., Mason, R.B. (1987) ″The Surface Treatment and Finishing of Aluminium and Its Alloys″, *Journal of The Electrochemical Society*, Vol. 104(8), DOI: 10.1149/1.2428628.

[14] Henley, V.F. (1982) ″*Anodic oxidation of aluminium and its alloys*″, Oxford, The Pergamon Materials Engineering Practice Series, U.K.

[15] Arrabal, R., Matykina, E., Hashimoto, T., Skeldon, P., Thompson, G.E. (2009) ″Characterization of AC PEO coatings on magnesium alloys″, *Surface and Coatings Technology*, Vol. 203(16), pp. 2207-2220.

[16] Bertuccioli, C., Garzoni, A., Martini, C., Morri, A., Rondelli, G. (2019) ″Plasma Electrolytic Oxidation (PEO) Layers from Silicate/Phosphate Baths on Ti-6Al-4V for Biomedical Components: Influence of Deposition Conditions and Surface Finishing on Dry Sliding Behaviour″, *Coatings*, Vol. 9(10), p. 614, https://doi.org/10.3390/coatings9100614

[17] Zehra, T., Kaseem, M., Hossain, S., Ko, Y.-G. (2021) ″Fabrication of a Protective Hybrid Coating Composed of TiO_2, MoO_2, and SiO_2 by Plasma Electrolytic Oxidation of Titanium″, *Metals*, Vol. 11, p. 1182, https://doi.org/10.3390/met11081182

[18] Mashtalyar, D., Imshinetskiy, I., Nadaraia, K., Gnedenkov, A., Sinebryukhov, S., Ustinov, A., Samokhin, A., Gnedenkov, S. (2022) ″Influence of ZrO_2/SiO_2 nanomaterial incorporation on the properties of PEO layers on Mg-Mn-Ce alloy″, *Journal of Magnesium and Alloys*, Vol. 10(2), pp. 513-526